

Dual-imaging-mode smart hydrogel information platform for illumination-independent covert decryption and read

Junjie Wei, Long Li, Rui Li, Qingquan Liu, Zejun Yan & Tao Chen

To cite this article: Junjie Wei, Long Li, Rui Li, Qingquan Liu, Zejun Yan & Tao Chen (2022) Dual-imaging-mode smart hydrogel information platform for illumination-independent covert decryption and read, International Journal of Smart and Nano Materials, 13:4, 612-625, DOI: [10.1080/19475411.2022.2116737](https://doi.org/10.1080/19475411.2022.2116737)

To link to this article: <https://doi.org/10.1080/19475411.2022.2116737>



© 2022 The Author(s). Published by Informa UK Limited, trading as Taylor & Francis Group.



[View supplementary material](#)



Published online: 31 Aug 2022.



[Submit your article to this journal](#)



Article views: 1457



[View related articles](#)



[View Crossmark data](#)



Citing articles: 1 [View citing articles](#)

Dual-imaging-mode smart hydrogel information platform for illumination-independent covert decryption and read

Junjie Wei^{a,b}, Long Li^{a,b}, Rui Li^{a,b}, Qingquan Liu^c, Zejun Yan^d and Tao Chen^{a,b}

^aKey Laboratory of Marine Materials and Related Technologies, Zhejiang Key Laboratory of Marine Materials and Protective Technologies, Ningbo Institute of Materials Technology and Engineering, Chinese Academy of Sciences, Ningbo, China; ^bSchool of Chemical Sciences, University of Chinese Academy of Sciences, Beijing, China; ^cHunan Provincial Key Laboratory of Advanced Materials for New Energy Storage and Conversion, Hunan University of Science and Technology, Xiangtan, China; ^dDepartment of Urology & Nephrology, Ningbo First Hospital, the Affiliated Hospital of Zhejiang University, Ningbo, China

ABSTRACT





Smart hydrogel with color responsiveness is envisioned as one of the most promising materials for advanced information encryption and decryption platform, but the illumination-dependent way of decrypting and reading information leads to the worrying of concealment in some particular scenarios. Herein, we proposed a smart hydrogel information platform with dual imaging modes by utilizing the accompanying behaviors in transparency change and heat releasing after crystallization of supercooled solution. For this smart hydrogel information platform, the hidden information could be written and decrypted by ink of ethylene glycol and decryption tool of seed crystal, respectively. Furthermore, in addition to the traditional optical imaging mode with the assistance of light illumination, the decrypted information on dual-imaging-mode hydrogel platform also could be read by thermal imaging mode in dark environment owing to the exothermic crystallization. The illumination-independent read mode based on heat radiation helps to improve the secrecy and safety of the decryption and read process. This investigation provides a facile and feasible strategy to design illumination-independent information platform that enables reading the encrypted information in secret.


ARTICLE HISTORY

Received 12 July 2022
Accepted 14 August 2022

KEYWORDS

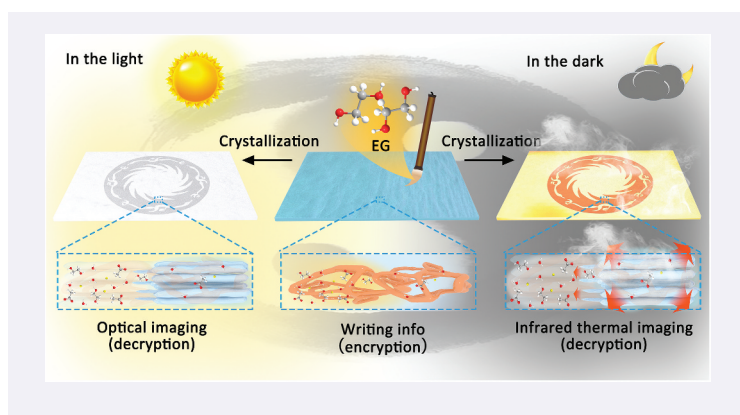
Hydrogel information platform; information decryption; thermal imaging; illumination-independent; pattern crystallization

CONTACT Tao Chen  tao.chen@nimte.ac.cn  Key Laboratory of Marine Materials and Related Technologies, Zhejiang Key Laboratory of Marine Materials and Protective Technologies, Ningbo Institute of Materials Technology and Engineering, Chinese Academy of Sciences, Ningbo 315201, China; Zejun Yan  yanzejun2000@sina.com  Department of Urology & Nephrology, Ningbo First Hospital, The Affiliated hospital of Zhejiang University, Ningbo 315010, China

 Supplemental data for this article can be accessed online at <https://doi.org/10.1080/19475411.2022.2116737>

© 2022 The Author(s). Published by Informa UK Limited, trading as Taylor & Francis Group.

This is an Open Access article distributed under the terms of the Creative Commons Attribution License (<http://creativecommons.org/licenses/by/4.0/>), which permits unrestricted use, distribution, and reproduction in any medium, provided the original work is properly cited.



1. Introduction

With the arrival of information age, the security of information, which has been related to all areas of society, plays an increasingly significant role in people's lives, social stability, and even national security [1–3]. For preventing the leakage of confidential information and constructing a secure environment, various novel information recording materials (e.g. dyes, magnetic materials, luminescent materials, and photonic crystal) [4–8] and encryption/decryption technologies (e.g. markers, laser holography, luminescent pattern, and security codes) [9–13] have flourished vigorously in the past decades, which have been extensively applied in anti-counterfeiting, privacy protection, and communication security. Compared to the traditional materials used for static single-dimension information, stimuli-responsive materials, which are capable of changing their physico-chemical properties in response to external stimuli, have attracted tremendous attention in the field of information encryption/decryption due to the higher level of information security and the bigger capacity of information storage [14].

As one of the most promising stimuli-responsive materials, smart hydrogel is envisioned as a superior candidate for information encryption/decryption owing to its compelling advantages in modifiability and multi-responsiveness [15–17]. Utilizing the adjustable optical properties, including the dynamic chemical colors and physical colors under UV and/or visible light irradiation [18–22], stimuli-responsive smart hydrogel has been widely applied as an advance information security platform. For example, Zhao's group reported a photoresponsive luminescence hydrogel based on the FRET behavior between lanthanide and photochromic units under alternating UV and visible light irradiation, realizing reversible multiple information encryption and decryption [20]. In addition to chemical colors like fluorescence and phosphorescence, physical colors based on reflection, absorption, and scattering also show great potential in high-security-level information. Liu et al. developed a 'double locking encryption system' by employing two types of thermo-responsive hydrogels with LCST and UCST phase behaviors, and the correct information with physical color can only be read within a specific temperature and time range [23]. Recently, more efficient strategies, such as multi-encryption with reconfigurable 3D shape [24,25] and transient information storage with self-erasing capacity [26–28], are proposed in order to further improve the security level of hydrogel platform.

However, the decrypted information based on both chemical colors and physical colors only can be read under light irradiation (visible light or UV light), resulting in a shortcoming in the concealment of information decryption and read process, which is crucial to getting information safely and secretly, especially for lurker and spy. Therefore, it is significant yet rather challenging to develop new stimuli-responsive hydrogel information platform for reading the encrypted information in secret.

Nature provides endless inspiration and ingenious paradigms for us. Bats are active at night without any light, but can see their surroundings clearly relying on the unique ability of thermal imaging [29,30]. Infrared thermal imaging technology can translate the temperature of object's surface to a visual image in the absence of light [31], providing a potential method to read information in secret. Interestingly, salt crystallization can not only change the transparency of object due to the generated crystals, but also change the temperature of object due to the exothermic behavior, realizing the simultaneous change of optical and thermal properties [32,33]. Inspired by the secrecy of infrared thermal imaging and the multi-responsiveness of crystallization, we herein developed a dual-imaging-mode smart hydrogel platform for information encryption and decryption by pattern crystallization of supercooled salt within hydrogel. Because of the hydrogen bonding between ethylene glycol (EG) and sodium acetate trihydrate (SAT), there is a inhibition effect of EG on crystals growth of SAT, and pattern hydrogels with encrypted information can be obtained through adding EG pattern to the hydrogel filled with supercooling SAT by utilizing this inhibition effect. The changes of physical color and temperature map accompanied with pattern crystallization enable that the encrypted information can be read in different environment (including in the light and in the dark) by means of optical imaging technology and infrared thermal imaging technology, improving the secrecy of info decryption and read process.

2. Materials and methods

2.1 Materials

Acrylamide (AAM), N,N'-Methylenebisacrylamide (MBAA), Ammonium persulfate ($(\text{NH}_4)_2\text{S}_2\text{O}_8$, APS) were purchased from Aladdin Industrial Co., and Ethylene glycol (EG) and Sodium acetate trihydrate ($\text{CH}_3\text{COONa}\cdot 3\text{H}_2\text{O}$, SAT) were purchased from Sinopharm Chemical Reagent Co., Ltd.

2.2 Preparation of the dual-imaging-mode smart hydrogel with various EG content

Typically, the dual-imaging-mode smart hydrogel was prepared as the following steps: First, 150 mg AAM, 1.5 mg MBAA, and a certain amount of EG (20, 40, 60, 80, 100 μL) were dissolved in the molten SAT liquid at 60°C with continuous stirring, forming the mixed solution containing 2 wt%, 4 wt%, 6 wt%, 8 wt%, and 10 wt% EG. Then, 5 mg APS was dissolved uniformly in the above mixed solution, and the mixed solution was poured into a mold rapidly before polymerization. Finally, the hydrogels with high-content of salt and various EG content were polymerized by thermal-initiation polymerization at 70°C for 5 min, and the supercooled dual-imaging-mode smart hydrogels with various EG content were obtained when the hydrogels were cooled to room temperature. When the supercooled hydrogels were touched by SAT

seed crystal, the crystallized dual-imaging-mode smart hydrogels were obtained after full crystallization.

2.3 Process of information encryption and decryption based on dual-imaging-mode smart hydrogel

The 2 wt% EG based dual-imaging-mode smart hydrogel film with 0.5 mm thickness was placed on a heater of 60°C, and the EG liquid was added on the surface of the hydrogel film through various methods, including squeezing a sponge filled with EG liquid, pouring EG liquid with the assistance of PET mask, and writing by a writing brush filled with EG liquid, ensuring the EG liquid covered on the surface of the hydrogel film forms an expected pattern and information. After standing for 2.5 min, the excess EG liquid was removed from the hydrogel film, and the dual-imaging-mode smart hydrogel with encrypted information was obtained after cooling. When the SAT seed crystal touched the encrypted hydrogel film, the hydrogel film was triggered to patterned crystallization, and the encrypted information on the hydrogel film was decrypted successfully. The decrypted information could be observed by naked eye in the light through optical imaging mode or infrared camera (Optris PI, Germany) in the dark through infrared thermal imaging mode.

3. Results and discussion

Introducing the supercooled salt into the hydrogel system is the key to prepare the dual-imaging-mode smart hydrogel. As shown in [Figure 1\(a,b\)](#), the dual-imaging-mode smart hydrogel was prepared through the following steps. First, the SAT was molten at 60°C, and the monomer (acrylamide), crosslinker (N,N'-Methylenebisacrylamide), thermal initiator (ammonium persulfate), and a certain amount of EG were dissolved in the molten SAT under magnetic stirring, forming the precursor solution with various content of EG (2 wt %, 4 wt%, 6 wt%, 8 wt%, 10 wt%) ([Figure 1a](#)). Then the precursor solution was placed in an oven (70°C) for polymerization, and a transparent hydrogel with high content of sodium acetate was prepared after 5 min. When the polymerized hydrogel cooled down naturally to room temperature, it was difficult for sodium acetate to spontaneously form crystal nucleus due to the high nucleation energy barrier, and thus the dual-imaging-mode smart hydrogel containing supercooled SAT was obtained successfully ([Figure 1b](#)). Owing to the metastability of the supercooled SAT within hydrogel, the supercooled SAT was triggered to crystal rapidly when a seed crystal (i.e. SAT particle) touched the surface of smart hydrogel, and a white hydrogel full of SAT crystals was obtained ([Figure 1c](#)). It is worth noting that the crystallization process triggered by seed crystal is exothermic, resulting in a significant change in temperature of hydrogel. Intriguingly, the SAT crystals within hydrogel can be easily molten again at high temperature (above 60°C). Accordingly, the dual-imaging-mode smart hydrogel can be regenerated through heating and natural cooling the crystallized hydrogel ([Figure 1b](#)). Benefitting from the responsiveness in transparency and temperature under stimulation from seed crystal, the smart hydrogel possesses great potential in the application of information encryption and decryption, realizing reading the information in dual modes, including optical imaging mode and infrared thermal imaging mode, which is suitable for the light and dark environment, respectively ([Figure 1d](#)).

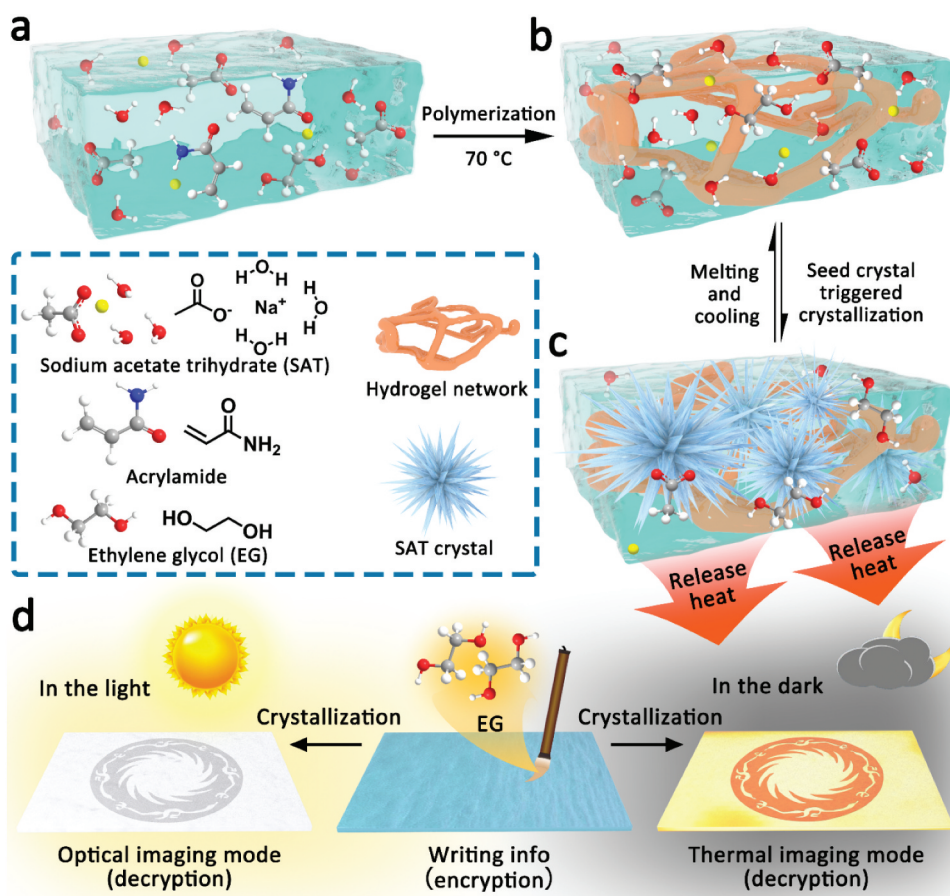


Figure 1. Schematic diagram of the dual-imaging-mode smart hydrogel based information platform. (a) Precursor solution of the dual-imaging-mode smart hydrogel. (b) Dual-imaging-mode smart hydrogel with supercooled salt solution. (c) Crystallized smart hydrogel after seed crystal triggered crystallization. (d) Application in information encryption and decryption platform by optical imaging mode and thermal imaging mode.

For proofing the stimuli-responsive behavior of the dual-imaging-mode smart hydrogel, a fish-shape hydrogel containing supercooled salt was prepared. As shown in Figure 2a, the fish-shape hydrogel with 2 wt% EG content was transparent and stable before receiving stimulation. However, once the SAT seed crystal touched the transparent hydrogel, a white region occurred instantaneously at the point of touch and spread throughout the entire hydrogel rapidly due to the confined crystallization of supercooled SAT within polymer matrix and the light scattering of generated SAT crystals, getting an all-white fish-shape crystallized hydrogel. When the crystallized hydrogel was heated on a heater of 70 °C, the white region faded away slowly along with the melting process of SAT crystals, and the transparent region eventually extended from the bottom position (high-temperature position due to contact with the heater) to the entire hydrogel. Besides, the crystallization process and melting process of the smart hydrogel were observed by a polarizing microscope. As shown in Figure 2b and Video S1, the needle

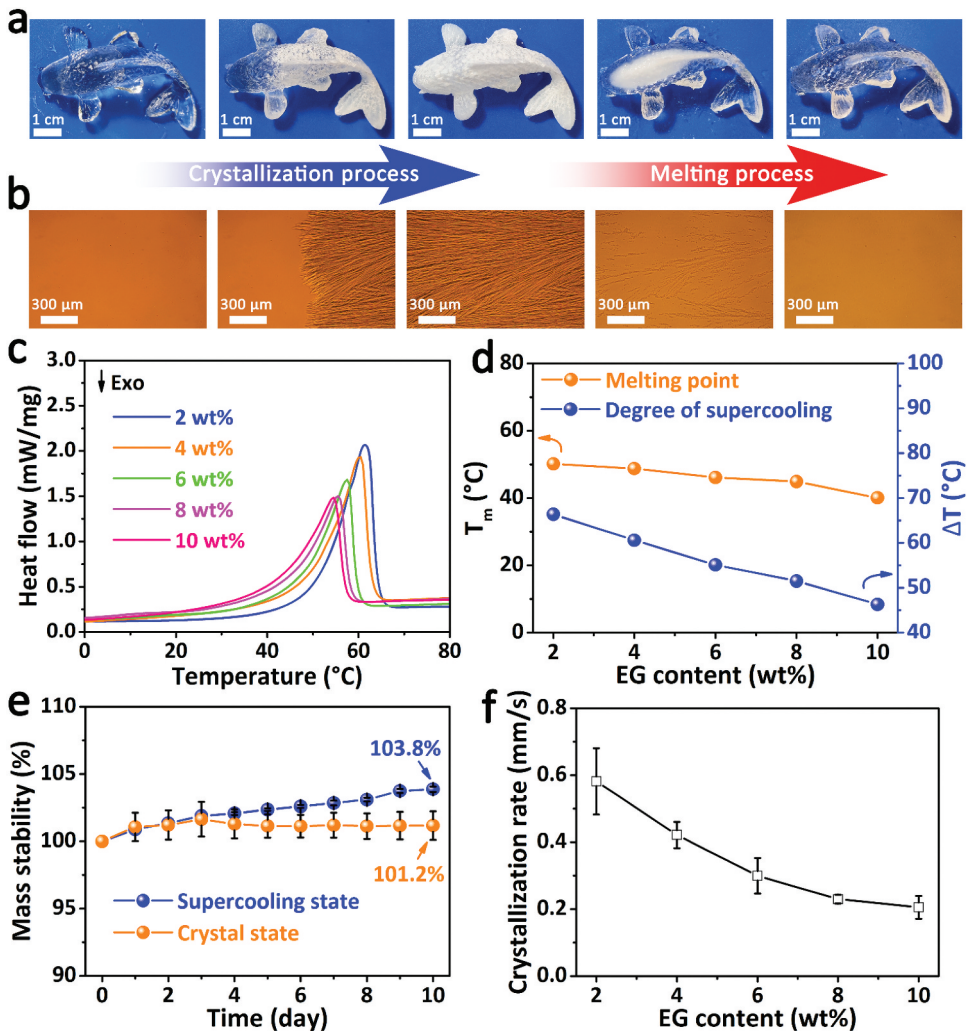


Figure 2. Crystallization behaviors of the dual-imaging-mode smart hydrogel. (a) Photos showing the crystallization and melting process of the smart hydrogel. (b) Crystallization and melting process of the 2 wt% EG based smart hydrogel by polarization microscope, the melting temperature is 70°C. (c) DSC curves of the smart hydrogel with various EG content at heating rate of 5°C/min. (d) Relation of EG content of the smart hydrogel to melting point and degree of supercooling. (e) Mass variations of the 2 wt% EG-based smart hydrogels with supercooling state and crystal state in an open natural environment. (f) Relationship between EG content of the smart hydrogel and crystallization rate.

SAT crystals grew quickly within hydrogel when the supercooled hydrogel was touched by seed crystal, and the needle crystals melted away gradually after being heated. The growing and melting behaviors of the SAT crystals are consistent with the changes in hydrogel's transparency, confirming the responsive color change of the smart hydrogel is derived from the SAT crystals.

The supercooling properties of the smart hydrogel with various EG content were measured by thermal analysis through the Differential Scanning Calorimetry (DSC). As the EG content increased from 2 wt% to 10 wt%, the solid-liquid transition temperature

(melting temperature) of the crystallized hydrogel decreased from 50.2°C to 40.1°C (Figure 2c), while the liquid-solid transition temperature (crystallization temperature) of the hydrogel increased from −16.2°C to −6.2°C (Figure S1). Therefore, the smart hydrogel can maintain the metastable supercooling state in a wide temperature range owing to its high degree of supercooling, but note that the EG will reduce the degree of supercooling of the SAT solution (Figure 2d). Although the smart hydrogel can switch freely between the two states under stimulation of seed crystal and high temperature, both supercooling state and crystal state are relatively stable. As shown in Figure 2e, the 2 wt% EG hydrogels in two states were placed in an open natural environment for 10 days, and there were only slight increment of 3.8% and 1.2% in weight for supercooling state and crystal state, respectively. When the EG content of hydrogel increased to 10 wt%, their weight changes only increased marginally to 5.5% and 2.8% due to the water absorption of EG (Figure S2). In addition to the degree of supercooling and stability, the EG content also affects the crystallization rate of the smart hydrogel. As shown in Figure 2f, the crystallization rate decreased from 0.6 mm/s to 0.2 mm/s as the EG content increased from 2 wt% to 10 wt%. Furthermore, the smart hydrogel showed satisfactory stability in the crystallization-heating cycles (Figure S3), ensuring its stability and reliability in application.

Obviously, there is specific interaction between ethylene glycol and sodium acetate trihydrate, which affects the physicochemical properties of SAT crystals. Therefore, the fourier transform infrared (FTIR) tests for SAT, EG, and SAT/EG mixture were carried out to reveal the mechanism. As shown in Figure 3a, after adding EG into SAT, the absorption band (in the range of 3500–3200 cm^{-1}) assigned to the O-H stretching vibration of crystal water is broadened, and shifts to lower wavenumber because of the reduction of force constant and the increase of dipole moment [34,35], suggesting a large number of hydrogen bonds are formed among EG

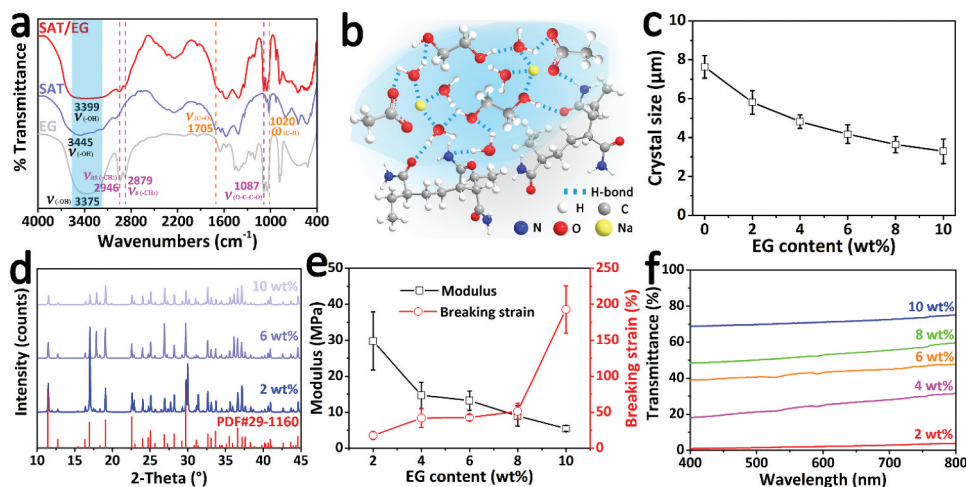


Figure 3. Inhibition effect of EG on SAT crystals growth. (a) FTIR spectrums of EG, SAT, and SAT/EG mixture. (b) Possible mechanism between SAT and EG in the supercooled smart hydrogel. (c) Relationship between EG content of the smart hydrogel and crystal size. (d) XRD spectrums of the smart hydrogel with various EG content. (e) Relation of EG content to the modulus and breaking strain of the smart hydrogel. (f) Transmittance curves of the smart hydrogel with various EG content in the visible wavelength range of 400–800 nm.

molecule and SAT molecule. For the spectrum of SAT, the peak at 1705 cm^{-1} is caused by the C=O stretching mode [36]. Besides, the characteristic peaks at 2946 cm^{-1} , 2879 cm^{-1} , and 1087 cm^{-1} in the spectrum of EG are ascribed to the asymmetrical stretching vibration, symmetrical stretching vibration of CH_2 , and the stretching vibration of O-C-C-O, respectively [37]. Interestingly, except for the O-H stretching vibration band, the spectrum of the SAT/EG mixture was a combination of the peaks of SAT and EG, indicating that there only existed hydrogen bonds between the components without the production of chemical reaction. According to the results of FTIR, the possible mechanism between EG and SAT crystals can be explained by the H-bonding interaction (Figure 3b). Due to the hydrogen bonds, the EG molecules will be adsorbed to the surface of SAT crystals in the crystallization process, inhibiting the growth of SAT crystals to some extent and reducing the crystallization rate of the supercooled hydrogel. This inhibition effect on SAT crystals growth was proved by the change in SAT crystal size. As shown in Figure 3c and S4, with the EG content increased from 0 wt% to 10 wt%, the diameter of SAT crystal gradually decreased from $7.6\text{ }\mu\text{m}$ to $3.3\text{ }\mu\text{m}$. The crystallized hydrogel with various EG content were determined using X-Ray Diffraction (XRD). As shown in Figure 3d, the XRD patterns of the crystallized hydrogels were matched with the diffraction peaks of SAT crystal (PDF#29-1160), and there were no remarkable changes in the diffraction peak positions for different EG content. However, the relative peak intensities of XRD patterns declined with the increasing EG content, meaning the crystallinity of SAT crystals decreased with the addition of EG, which confirmed the inhibition effect of EG again.

Intriguingly, the size and crystallinity of SAT crystals have a profound effect on the mechanical properties and optical properties of the smart hydrogel. The crystallization of supercooled solution within hydrogel can greatly enhance the mechanical properties of hydrogel due to the formation of high-strength SAT crystals that was proved by previous studies [32,38]. As shown in Figure 3e and S5, thanks to the effect of EG on the SAT's crystallinity, there was a negative correlation between the modulus of the crystallized hydrogel and EG content, but the crystallized hydrogel still reached a big value of modulus (5.5 MPa) when the EG content was 10 wt%, much greater than that of the supercooled hydrogel (<15 kPa) (Figure S6). Additionally, the breaking strain of the crystallized hydrogel was positively correlated with the EG content. Because of the scattering of light by SAT crystals, the physical color of the smart hydrogel transforms from colorless and transparent to white during the crystallization process. Therefore, the transparency of the crystallized hydrogel can be adjusted by controlling the size of SAT crystals through adding EG. As a demonstration, we compared the transparency of the crystallized hydrogel with various EG content. It is obvious that the higher the EG content, the better the transparency (Figure S7). Furthermore, the ultraviolet-visible spectrophotometer was employed to quantitatively analyze the transmittance. As shown in Figure 3f, the transmittance of the crystallized hydrogel in the visible wavelength range improved dramatically when the EG content was increased from 2 wt% to 10 wt%. The significant difference in transparency provides a good foundation for building the hydrogel based information encryption and decryption platform using EG.

In order to proofing the feasibility of building the hydrogel information platform based on transparency difference, the 2 wt% supercooled hydrogel film and the EG were acted as 'paper' for loading information and 'ink' for writing information, respectively (Figure 4a). The supercooled hydrogel film containing local high-content EG pattern was prepared by controlling the distribution area of EG through adding extra EG liquid. Under the stimulation of seed crystal, the low-content EG region and the high-content EG region crystallize at different rates,

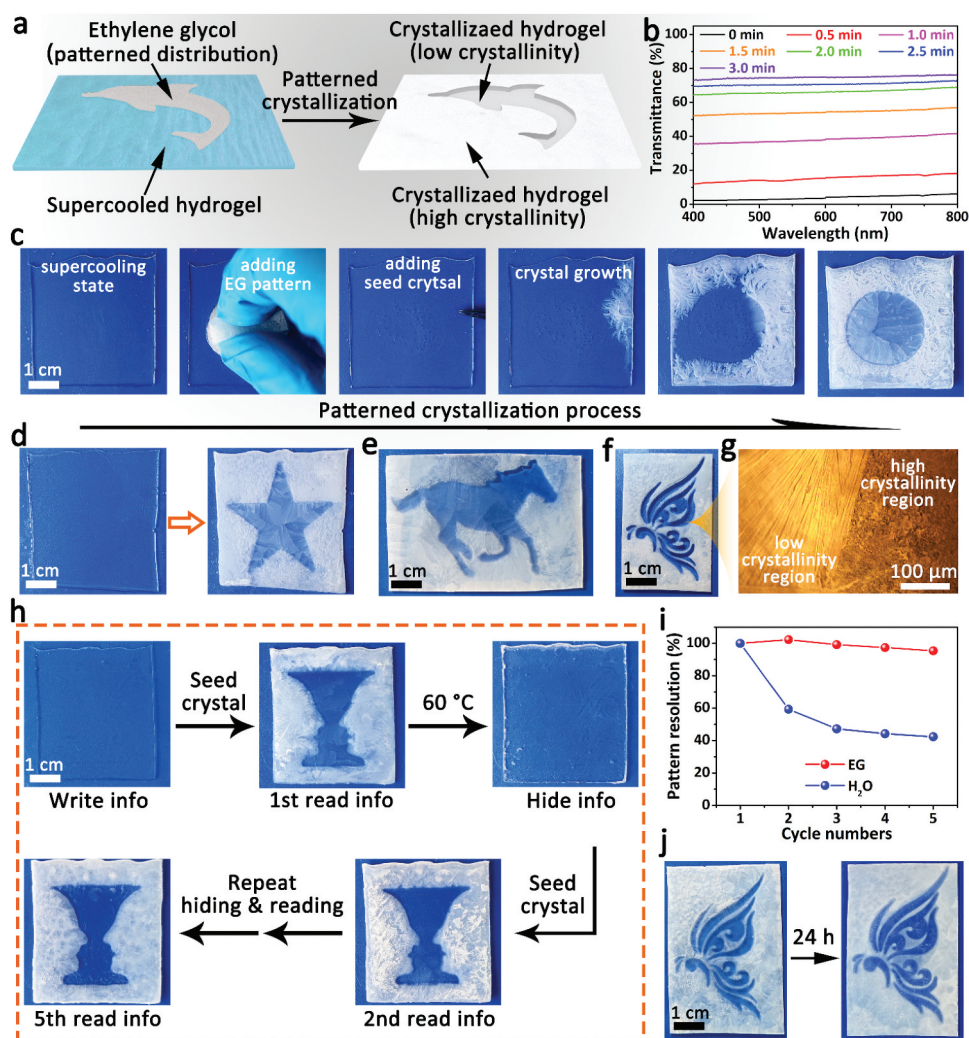


Figure 4. Hydrogel based information platform in optical imaging mode under light illumination. (a) Scheme of the hydrogel-based information platform using EG ink. (b) Influence of EG diffusion time on the transparency of the crystallized smart hydrogel film with 0.5 mm thickness. (c) Photos showing the pattern crystallization process of the smart hydrogel after adding circular EG pattern. (d-f) Photos showing patterned crystallized hydrogel films containing patterns of (d) pentagram, (e) horse, and (f) butterfly under the assistance of PET mask and EG ink. (g) Microscopic image of the boundary of the patterned hydrogel by polarization microscope. (h) Photos showing cyclic information encryption and decryption process. (i) Comparison of EG ink and water ink on the cycle stability of pattern resolution. (j) Long-term stability of the patterned hydrogel in 24 h.

eventually getting the preset pattern with different crystallinities and transparencies. Actually, the introduction of external EG into the supercooled hydrogel relies on the diffusion of EG before crystallization; thus, the diffusion time affects the EG content and the final transparency greatly. For determining the appropriate diffusion time, the relationship between the diffusion time and the final transparency of the crystallized hydrogel film (0.5 mm thickness) was investigated. As shown in Figure 4b, when the diffusion time is less than 2 min, the

transmittances of the crystallized hydrogel film were improved sharply, but maintained a relatively stable value in the subsequent time. Hence, the diffusion time was determined as 2.5 min in the following study. As a demonstration, a circular EG pattern was added into the 2 wt% supercooled hydrogel film as preset information through squeezing the sponge stamp filled with EG and later standing for 2.5 min, and the circular pattern was obtained finally after differentiating crystallization (Figure 4c, Video S2). Besides, with the assistance of PET mask containing hollowed-out patterns, more elaborate and complicated patterns could be achieved readily by using this strategy, such as pentagram, horse, and butterfly (Figure 4d-f). The interface between different regions was observed by polarizing microscope. As shown in Figure 4g, there was a clear boundary between the high-crystallinity region and low-crystallinity region, revealing that this pattern based on supercooled hydrogel film and EG possesses a high accuracy, which is crucial to ensure the correctness and readability of the encrypted information.

Furthermore, the supercooled hydrogel film was applied as the optical imagery-based information encryption and decryption platform using the above method. As shown in Figure 4h, the preset information was written on the supercooled hydrogel platform by the EG ink, and the encrypted information was invisible. For decrypting the invisible information, a seed crystal of SAT was employed as decryption tool. After seed crystal triggered crystallization, the encrypted information rapidly displayed on the hydrogel platform. What is more, the decrypted information could be hid again through heating the crystallized hydrogel platform, and the 2nd decryption and read also could be realized by seed crystal. Surprisingly, although undergo repeated hiding and reading, the decrypted information was still clear and readable (Figure S8). In addition to EG, water also can act as 'ink' to write the information by dissolving SAT crystals, but the displayed pattern is unstable during the hiding-reading cycles due to the high diffusivity of water molecule (Figure S9). For quantifying the clarity of pattern information, we proposed a new parameter – 'pattern resolution,' which is defined as S/L^2 , where the S and L are the area and perimeter of the pattern, respectively. As shown in Figure 4i, the pattern resolution of the EG-ink-based information only dropped slightly (~4.6%) after 5 cycles, much lower than that of water based information (~57.7%). Additionally, it was a pleasant surprise to find the decrypted information remained clear even after standing for 24 h (Figure 4j). The amazing stability of the optical-imagery-based hydrogel information platform improved its practicability and reliability.

SAT is a kind of phase change materials with high enthalpy of latent heat, and the crystallization of supercooled SAT solution is accompanied by the release of latent heat because the lattice energy is less than the hydration energy. Therefore, the smart hydrogel containing the supercooled SAT also possesses the similar responsive exothermal behavior after crystallization. As shown in Figure 5a, the dynamic temperature maps of the supercooled hydrogel with various EG content were recorded by infrared camera. Due to the quick release of latent heat, the maximum temperature of the entire smart hydrogel with 2 wt% EG rapidly increased from ambient temperature to ~47.7°C in 60 s, while the 10 wt% EG-based smart hydrogel only increased to 34.2°C due to the lower crystallization rate and slower heat accumulation (difference value between obtained heat and dissipated heat). After the temperature reached the highest value, it dropped slowly as the dissipation of heat. Besides, the real-time temperature of the initial crystallization position in the smart hydrogel shows a similar phenomenon. As shown in Figures 5 b and c, the maximum raised temperature (ΔT) and heating rate at the initial crystallization position

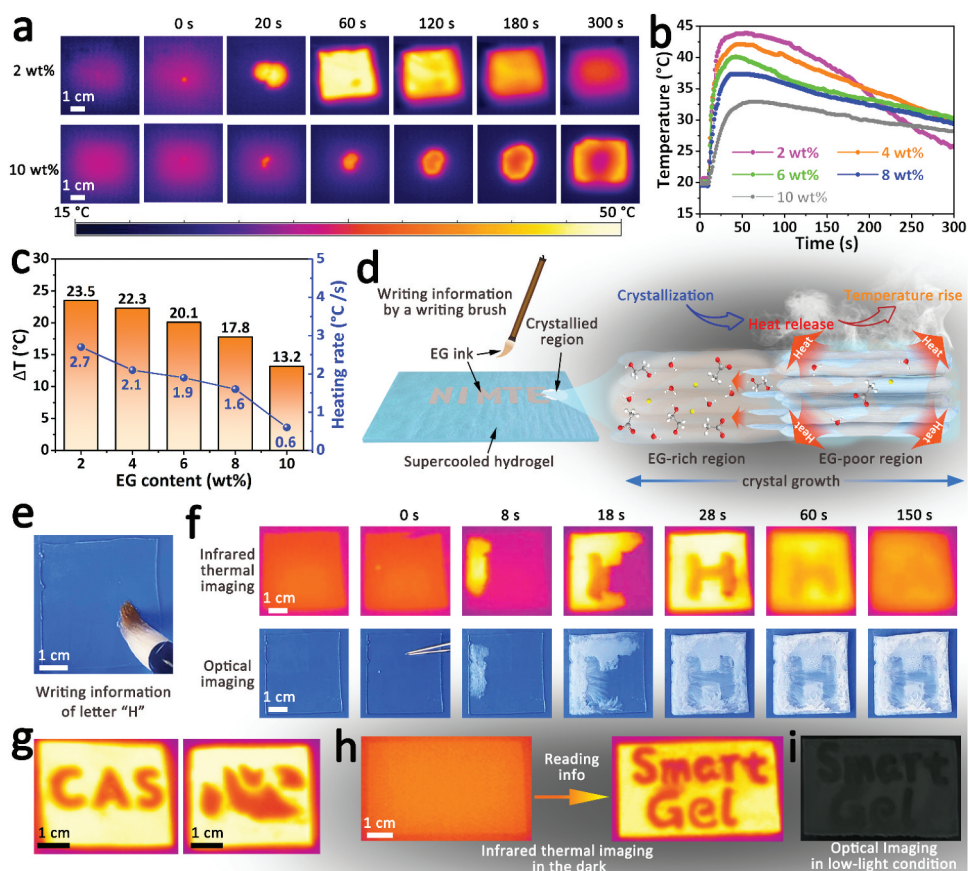


Figure 5. Hydrogel-based information platform in infrared thermal imaging mode in the dark. (a) Time-dependent infrared thermal images of the smart hydrogel (0.5 mm in thickness) with various EG content during crystallization process. (b) Real-time temperature curves of the initial crystallization position in the smart hydrogel with various EG content. (c) Relation of EG content to the maximum increased temperature and heating rate of the smart hydrogel during crystallization process. (d) Scheme of the mechanism of the hydrogel based information platform using EG ink. (e) Photo showing writing letter 'H' on hydrogel film by a writing brush with EG ink. (f) Information decryption and read process in infrared thermal imaging mode and optical imaging mode. (g) Reading the decrypted information of 'CAS' and '♡' by infrared thermal imaging mode. (h-i) Reading the decrypted information of 'Smart Gel' by (h) infrared thermal imaging mode in the dark and (i) optical imaging mode in low-light condition.

decreased gradually as the increasing EG content because of the influence from crystallization rate. This great difference in hydrogel's temperature exhibits a potential application in thermal-imagery-based information platform.

As shown in Figure 5d, the structure of the thermal-imaging-based information platform is same as that of optical-imaging-based information platform, but the mechanism for information display is infrared thermal imaging. The adding of EG ink leads to a differential distribution of EG content, resulting in the different crystallization rate and temperature distribution, which can be observed by infrared camera using thermal imaging technology. For example, an information of letter 'H' was written on

the supercooled hydrogel film by a writing brush (Figure 5e, Video S3), and the encrypted information 'H' could be read through both infrared thermal imaging technology and optical imaging technology after crystallization (Figure 5f). What is even more interesting is that the decrypted information displayed by infrared thermal imaging was then automatically erased within 2 min because of the inevitable heat exchange and heat dissipation. This time-dependent self-destruction ability after decryption contributes to improve the security level of the hydrogel-based information platform. Besides, the use of writing brush can greatly improve the convenience and practicability of encryption, writing complex information without the assistant of mask (Figure 5g). Of greater significance, the thermal-imagery-based information platform can be used in dark environment. As shown in Figure 5h, the encrypted information on the dual-imaging-mode smart hydrogel platform could be read through infrared thermal imaging technology without any light irradiation, but this is an impossible task to read information by optical imaging in the dark (Figure S10). The encrypted information can only be read with the assistance of indispensable light (Figure 5i). During the decryption process, this information platform built by dual-imaging-mode smart hydrogel emits no light and does not require external light, providing a secretive way to decrypt and read hidden information, which is helpful to guarantee the concealment and safety of the person in need of decrypting secretly.

4. Conclusion

In summary, utilizing the changes in transparency and temperature during crystallization process, a smart hydrogel information platform with both optical imaging mode and thermal imaging mode was developed through introducing supercooled salt solution into hydrogel matrix. Under the stimulation from seed crystal, the metastable supercooling solution within hydrogel was triggered to crystal rapidly, resulting in the reduction of transparency and the release of latent heat due to the light scattering of SAT crystals and the low lattice energy. Owing to its inhibition effect on crystals growth, EG was employed as ink to write hidden information on the smart hydrogel information platform, and then the encrypted information based on crystallinity difference could be decrypted by pattern crystallization and read by optical imaging technology in the light. More significantly, due to the difference in the rate of crystallization and heat accumulation, there is a temperature map relied on temperature difference with spatial resolution for the decrypted information, which could be read through infrared thermal imaging technology even in darkness. This illumination-independent read method contributes to improve the concealment of decrypting and reading information. Therefore, the dual-imaging-mode smart hydrogel provides a new strategy for building advanced hydrogel-based information encryption and decryption platform, and exhibits a profound potential in illumination-independent decryption, which is crucial to obtain information secretly.

Disclosure statement

No potential conflict of interest was reported by the authors.

Funding

This work was supported by the China Postdoctoral Science Foundation [2021M690157,2022T150668]; National Natural Science Foundation of China [52103152]; Ningbo Natural Science Foundation [2121J206].

References

- [1] Ren W, Lin GG, Clarke C, et al. Optical Nanomaterials and Enabling Technologies for High-Security-Level Anticounterfeiting. *Adv Mater.* 2020;32:1901430.
- [2] Wang H, Ji XF, Page ZA, et al. Fluorescent materials-based information storage. *Mater Chem Front.* 2020;4:1024.
- [3] Yang F, Ye SS, Dong WH, et al. Laser-Scanning-Guided Assembly of Quasi-3D Patterned Arrays of Plasmonic Dimers for Information Encryption. *Adv Mater.* 2021;33:2100325.
- [4] Li JT, Bisoyi HK, Lin SY, et al. 1,2-Dithienyldicyanoethene-Based, Visible-Light-Driven, Chiral Fluorescent Molecular Switch: Rewritable Multimodal Photonic Devices. *Angew Chem Int Ed.* 2019;58:16052.
- [5] Li JT, Bisoyi HK, Tian JJ, et al. Optically Rewritable Transparent Liquid Crystal Displays Enabled by Light-Driven Chiral Fluorescent Molecular Switches. *Adv Mater.* 2019;31:1807751.
- [6] Liu L, Shi JP, Li YA, et al. Disguise as fluorescent powder: Ultraviolet-B persistent luminescence material without visible light for advanced information encryption and anti-counterfeiting applications. *Chem Eng J.* 2022;430:132884.
- [7] Arsenault AC, Puzzo DP, Manners I, et al. Photonic-crystal full-colour displays. *Nat Photonics.* 2007;1:468.
- [8] She PF, Ma Y, Qin YY, et al. Dynamic Luminescence Manipulation for Rewritable and Multi-level Security Printing. *Matter.* 2019;1:1644.
- [9] Hu HB, Zhong H, Chen CL, et al. Magnetically responsive photonic watermarks on banknotes. *J Mater Chem C.* 2014;2:3695.
- [10] Kumar P, Singh S, Gupta BK. Future prospects of luminescent nanomaterial based security inks: from synthesis to anti-counterfeiting applications. *Nanoscale.* 2016;8(30):14297.
- [11] Ye WM, Zeuner F, Li X, et al. Spin and wavelength multiplexed nonlinear metasurface holography. *Nat Commun.* 2016;7:11930.
- [12] Li XP, Lan TH, Tien CH, et al. Three-dimensional orientation-unlimited polarization encryption by a single optically configured vectorial beam. *Nat Commun.* 2012;3:998.
- [13] Li B, Lin CL, Lu CJ, et al. A rapid and reversible thermochromic supramolecular polymer hydrogel and its application in protected quick response codes. *Mater Chem Front.* 2020;4:869.
- [14] Le XX, Shang H, Wu SS, et al. Heterogeneous fluorescent organohydrogel enables dynamic anti-counterfeiting. *Adv Funct Mater.* 2021;31(52):2108365.
- [15] Chen Z, Chen YJ, Guo YT, et al. Paper-structure inspired multiresponsive hydrogels with solvent-induced reversible information recording, self-encryption, and multidecryption. *Adv Funct Mater.* 2022;32(23):2201009.
- [16] Zhang YL, Li YS, Chen KX, et al. Body temperature triggered customized patterned thermo-sensitive hydrogel for information storage and display. *Polymer.* 2019;179:121637.
- [17] Wen HJ, Wang B, Zhu HB, et al. Security-enhanced 3D data encryption using a degradable pH-responsive hydrogel. *Nanomaterials.* 2021;11(7):1744.
- [18] Yang YB, Li QY, Zhang HW, et al. Codes in code: AIE supramolecular adhesive hydrogels store huge amounts of information. *Adv Mater.* 2021;33(45):2105418.
- [19] Ji XF, Wu RT, Long LL, et al. Encoding, reading, and transforming information using multi-fluorescent supramolecular polymeric hydrogels. *Adv Mater.* 2018;30(11):1705480.
- [20] Li ZQ, Chen HZ, Li B, et al. Photoresponsive luminescent polymeric hydrogels for reversible information encryption and decryption. *Adv Sci.* 2019;6(21):1901529.

- [21] Yu CT, Cui KP, Guo HL, et al. Structure frustration enables thermal history-dependent responsive behavior in self-healing hydrogels. *Macromolecules*. 2021;54(21):9927.
- [22] Yue YF, Haque MA, Kurokawa T, et al. Lamellar hydrogels with high toughness and ternary tunable photonic stop-band. *Adv Mater*. 2013;25(22):3106.
- [23] Lou DY, Sun YJ, Li J, et al. Double lock label based on thermosensitive polymer hydrogels for information camouflage and multilevel encryption. *Angew Chem Int Ed*. 2022;134(16):e202117066.
- [24] Zhu CN, Bai TW, Wang H, et al. Dual-encryption in a shape-memory hydrogel with tunable fluorescence and reconfigurable architecture. *Adv Mater*. 2021;33(29):2102023.
- [25] Shang H, Le XX, Sun Y, et al. Integrating photorewritable fluorescent information in shape-memory organohydrogel toward dual encryption. *Adv Opt Mater*. 2022;10(13):2200608.
- [26] Le XX, Shang H, Yan HZ, et al. A urease-containing fluorescent hydrogel for transient information storage. *Angew Chem Int Ed*. 2021;60(7):3640.
- [27] Yu CT, Guo HL, Cui KP, et al. Hydrogels as dynamic memory with forgetting ability. *Proc Natl Acad Sci U S A*. 2020;117(32):18962.
- [28] Deng SH, Huang LM, Wu JJ, et al. Bioinspired dual-mode temporal communication via digitally programmable phase-change materials. *Adv Mater*. 2021;33(24):2008119.
- [29] Gracheva EO, Cordero-Morales JF, Gonzalez-Carcacia JA, et al. Ganglion-specific splicing of TRPV1 underlies infrared sensation in vampire bats. *Nature*. 2011;476(7358):88.
- [30] Campbell AL, Naik RR, Sowards L, et al. Biological infrared imaging and sensing. *Micron*. 2002;33(2):211.
- [31] Meola C, Carlomagno GM. Recent advances in the use of infrared thermography. *Meas Sci Technol*. 2004;15(9):R27.
- [32] Wei JJ, Wei GM, Shang YH, et al. Dissolution–crystallization transition within a polymer hydrogel for a processable ultratough electrolyte. *Adv Mater*. 2019;31:1900248.
- [33] Schroeder TBH, Aizenberg J. Patterned crystal growth and heat wave generation in hydrogels. *Nat Commun*. 2022;13(1):259.
- [34] Cui YM, Zhu YY, Dai R, et al. The solubility and interactions of gelatin in “water-in-sodium acetate trihydrate/urea-DES” system. *Colloids Surf, A*. 2021;625:126916.
- [35] Li X, Fu ZH, Qiao YJ, et al. Preparation, characterization, and modification of sodium acetate trihydrate-urea binary eutectic mixtures as phase change material. *Energy Fuels*. 2020;34(5):6439.
- [36] Wong JIC, Ramesh S, Jun HK, et al. Development of poly(vinyl alcohol) (PVA)-based sodium ion conductors for electric double-layer capacitors application. *Mater Sci Eng B*. 2021;263:114804.
- [37] Guo YC, Cai C, Zhang YH. Observation of conformational changes in ethylene glycol–water complexes by FTIR–ATR spectroscopy and computational studies. *Aip Adv*. 2018;8(5):055308.
- [38] Yang F, Cholewinski A, Yu L, et al. A hybrid material that reversibly switches between two stable solid states. *Nat Mater*. 2019;18(8):874.